International Journal of Bio-Inorganic Hybrid Nanomaterials

Numerical Study of Furnace Temperature and Inlet Hydrocarbon Concentration Effect on Carbon Nanotube Growth Rate

Babak Zahed[1], Tahereh Fanaei Sheikholeslami[2*], Amin Behzadmehr[3], Hossein Atashi[4]

[1] *M.Sc., Mechanical Engineering Department, University of Sistan and Baluchestan, Zahedan, Iran*
[2] *Assistant Professor, Electrical and Electronic Department, University of Sistan and Baluchestan, Zahedan, Iran*
[3] *Professor, Mechanical Engineering Department, University of Sistan and Baluchestan, Zahedan, Iran*
[4] *Professor,Chemical Engineering Department, University of Sistan and Baluchestan, Zahedan, Iran*

ABSTRACT

Chemical Vapor Deposition (CVD) is one of the most important methods for producing Carbon Nanotubes (CNTs). In this research, a numerical model, based on finite volume method, is investigated. The applied method solves the conservation of mass, momentum, energy and species transport equations with aid of ideal gas law. Using this model, the growth rate and thickness uniformity of produced CNTs, in a horizontal CVD reactor, at atmospheric pressure, are calculated. The furnace temperature and inlet hydrocarbon concentration variations are studied as the effective parameters on CNT growth rate and thickness uniformity. It is indicated that by increasing the furnace temperature, the CNT growth rate increases, while the thickness uniformity shows decreasing. The results show that the growth rate of produced CNTs could be improved by increasing the inlet hydrocarbon concentration, but the latter causes more non uniformity on the CNTs height.

Keyword: CNT growth rate; CVD; Furnace temperature; Hydrocarbon concentration; Numerical analysis.

1. INTRODUCTION

Carbon nanotubes (CNTs) are tubular structures, formed by carbon atoms with the diameter in range of one to tens nanometer. After Iijima's discovery in 1991 [1] an extensive academic and industrial researches have been conducted on CNT, because of its interesting electrical, thermal and mechanical properties [2-5].

However, one of the most important issues in this field that must be well addressed is mass production and high cost production of CNT. Thus,

(*) Corresponding Author - e-mail: tahere.fanaei@ece.usb.ac.ir

Int. J. Bio-Inorg. Hybd. Nanomat., Vol. 2, No. 1(2013), 329-336

Zahed B et al

the researchers have examined different methods to produce high quality CNTs, easier and with lower cost. Among the various methods for CNT production, Chemical Vapour Deposition (CVD) due to its handling procedure, simplicity and possibility of high production rate is vastly used [6-8]. CNT growth rate in an atmospheric pressure CVD (APCVD) reactor depends on various parameters such as inlet flow rate, deposition temperature, inlet hydrocarbon concentration and catalyst types [9-11]. To obtain desired CNT growth rate and acceptable thickness uniformity, numerical analyses are used prior to experimental studies. Numerical studies can be used to investigate the effect of various conditions and also to help understanding the details of processes for well interpretation of different parameters such as growth rate, transport rates and reaction mechanisms. In this regard, Grujicic et al. [12] proposed a model, where the detailed gas-phase reactions of CH_4, surface reactions for CNT growth were contained. The growth rates of CNTs and also distribution of velocity, temperature and concentration under different growth conditions, were investigated. Also, Endo et al. [13] estab- lished a CFD model that predicted the production rate of nanotubes via catalytic decomposition of xylene in a CVD reactor. They predicted velocity and temperature distributions and concentration distributions in the reactor. Using this model, they calculated and measured the total production rates with various inlet xylene concentrations. Similar works were done with the other researchers to model the CNT growth rate with different deposition conditions [14-16].

The horizontal quartz tube reactor is a simple system which is vastly used in catalytic CVD. Two carrier gases that can be used are argon and nitrogen [16-18] with certain amount of hydrogen that added into carrier gas to prevent the oxidation of catalyst particles and the formation of other carbon impurities during the CNT production. The carbon sources can be in gas state (methane, acetylene, ethylene, etc) [19-25] or in liquid state (alcohol, benzene, toluene, xylene, etc.) [26-28].

In this research, a catalytic APCVD technique

for production of CNT is modelled, numerically. The inlet gas mixture includes xylene as carbon source and a mixture of argon with 10% hydrogen, as carrier gas. The effects of furnace temperature and inlet hydrocarbon concentration on growth rate and thickness uniformity has been studied and discussed.

2. PROBLEM DESCRIPTION

Ferrocene vapor with carrier gas (argon) is entered into a horizontal reactor that works at atmosphere pressure. A uniform layer of iron atoms on the furnace wall is considered as a catalyst for surface reaction. Therefore, inlet gas mixture including xylene (C_8H_{10}) and carrier gas (argon with 10% hydrogen), enters into reactor continuously. Reactor processes is modeled with two gas phase reactions and four surface reactions. These reactions release carbon atoms to produce CNTs on the catalyst particle that layout on the reactor hot walls.

3. GOVERNING EQUATIONS

Considering two dimensional axisymmetric model and steady state process, the governing equations are as follow:
Conservation of Mass:

$$\frac{\partial \rho}{\partial t} = -\nabla \cdot \left(\rho \vec{V} \right) \tag{1}$$

Conservation of Momentum:

$$\frac{\partial \rho \vec{V}}{\partial t} = -\nabla \cdot \left(\rho \vec{V} \vec{V} \right) + \nabla \cdot \tau - \nabla P + \rho \vec{g} \tag{2}$$

For Newtonian fluids such as existent gases in CVD reactors, viscous stress tensor is as follows:

$$\tau = \mu \left(\nabla \vec{V} + \left(\nabla \vec{V} \right)^T \right) + \left(k - \frac{2}{3}\mu \right) \left(\nabla \cdot \vec{V} \right) I \tag{3}$$

Zahed B et al

Int. J. Bio-Inorg. Hybd. Nanomat., Vol. 2, No. 1 (2013), 329-336

These equations are coupled with energy equation. Energy Equation:

$$C_p \frac{\partial \rho T}{\partial t} = -C_p \nabla.(\rho \vec{V} T) + \nabla.(\lambda \nabla T) +$$

$$\nabla \left(RT \sum_{i=1}^{N} \frac{D_i^T}{m_i} \nabla(\ln f_i) \right) + \sum_{i=1}^{N} \frac{H_i}{m_i} \nabla.\vec{J}_i -$$

$$\sum_{i=1}^{N} \sum_{k=1}^{K} H_i v_{ik} \left(R_k^g - R_{-k}^g \right) \qquad (4)$$

and Species Transport Equation:

$$\frac{\partial (\rho \omega_i)}{\partial t} = -\nabla. \left(\rho \vec{V} \omega_i \right) - \nabla.\vec{J}_i +$$

$$m_i \sum_{k=1}^{k} v_{ik} \left(R_k^g - R_{-k}^g \right) \qquad (5)$$

These equations solve subject to the following boundary conditions:

- Reactor walls are impermeable and no slip condition is considered for the velocity at walls.
- Constant temperature at the heated walls and zero heat flux at the adiabatic walls.
- At the nonreactant walls, mass flux vector for each species must be zero.
- Due to surface reactions, net mass production rate P_i for i^{th} gas specie at the surface of furnace is:

$$P_i = m_i \sum_{l=1}^{L} \sigma_{il} R_l^s \qquad (6)$$

Thus the normal velocity on the surface of furnace can be express by:

$$\vec{n}.\vec{V} = \frac{1}{\rho} \sum_{i=1}^{N} m_i \sum_{l=1}^{L} \sigma_{il} R_l^s \qquad (7)$$

Total net mass flux of ith specie, normal to the surface of furnace must be equal to P_i. Thus:

$$\vec{n}.\left(\rho \omega_i \vec{V} + \vec{J}_i^c + \vec{J}_i^T \right) = m_i \sum_{i=1}^{L} \sigma_{il} R_l^s \qquad (8)$$

4. NUMERICAL ANALYSIS

The governing equations are discretized using finite volume approach. SIMPLE algorithm is adopted for the pressure-velocity coupling.

Physical properties (viscosity, thermal conductivity and specific heat capacity) for each species are assumed to be thermal dependent [29]. These properties for the gas mixture were obtained using the mixing law.

Non-uniform structured grid distribution that is refined near walls is considered. Convergence criterion for energy equation is 10^{-10} and for other equations (continuity, momentum and species transport) is 10^{-6}.

5. MODELING

Tubular hot wall reactor that is worked at atmosphere pressure is modelled. It has 34 mm diameter and 1.5 meter length with 17 mm inlet/outlet diameter (Figure 1). Inlet gas mixture including xylene and argon with 10% hydrogen as carrier gas enters into the reactor. Its temperature and inlet mass flow rate are 300 K and 685 sccm (standard cubic centimeters per minute) respectively. Then inlet gas mixture is heated in preheater up to 513 K and then enters to the furnace region.
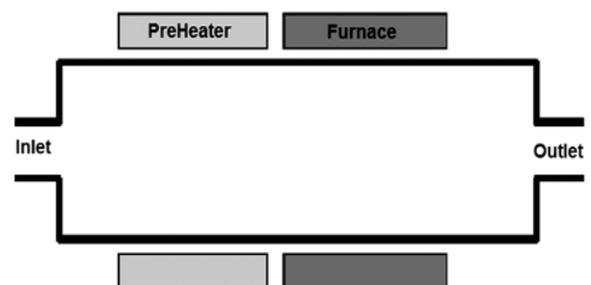

Figure 1: CVD Reactor Scheme.

Int. J. Bio-Inorg. Hybd. Nanomat., Vol. 2, No. 1 (2013), 329-336

Zahed B et al

Preheater zone is considered from 20 to 50 cm and furnace zone from 60 to 125 cm from the inlet section. Except of preheater and furnace walls that are isothermal walls, other walls are considered to be adiabatic. A schematic of the considered modelled is shown in Figure 1.

Reactions that is used in this model, is shown in Tables 1 and 2. There are two gas phase reactions and four surface reactions apply for this model. All reactions are irreversible. Also kinetic rate coefficients determined with no catalyst deactivation assumption.

Table 1: *Gas phase reaction [13].*

Gas Phase Reactions	PEF	AE	TE
$C_8H_{10}+H_2 \rightarrow C_7H_8+CH_4$	2.512e+8	1.674e+8	0
$C_7H_8 + H_2 \rightarrow C_6H_6+CH_4$	1.259e+11	2.2243e+8	0

Table 2: *Surface reactions [13].*

Gas Phase Reactions	PEF	AE	TE
$C_8H_{10} \rightarrow 8C + 5H_2$	0.00034	0	0
$C_7H_8 \rightarrow 7C + 4H_2$	0.00034	0	0
$C_6H_6 \rightarrow 6C + 3H_2$	0.00034	0	0
$CH_4 \rightarrow C + 2H_2$	0.008	0	0

PEF= Pre-Exponential Factor, AE= Activation Energy,

TE= Temperature Exponent

6. VALIDATION OF NUMERICAL RESULTS

Non-uniform structured grid, that is refined at the near walls where the gradient of the parameters are important, is selected. Several different grid distributions have been tested to ensure the results are grid independence. The selected grid number is 10998. In addition to show the accuracy of the results, comparisons are made between the obtained numerical results and numerical results of Endo et al. [13] for two different xylene concentrations. It is shown in Figure 2, as seen good concordance between the results is obtained (Maximum of error

5%). Thus the numerical procedure is reliable and can well predict the process throughout the reactor.
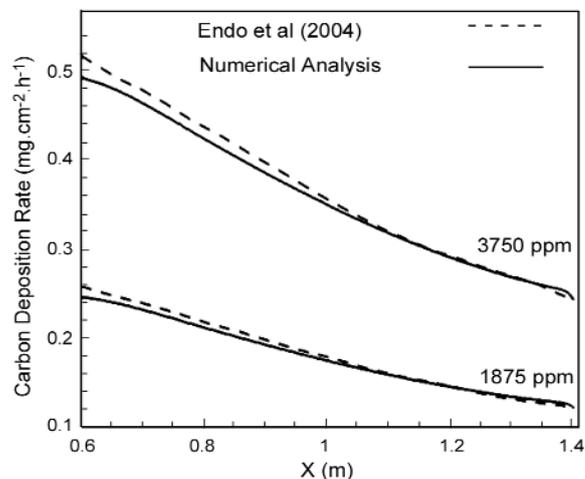

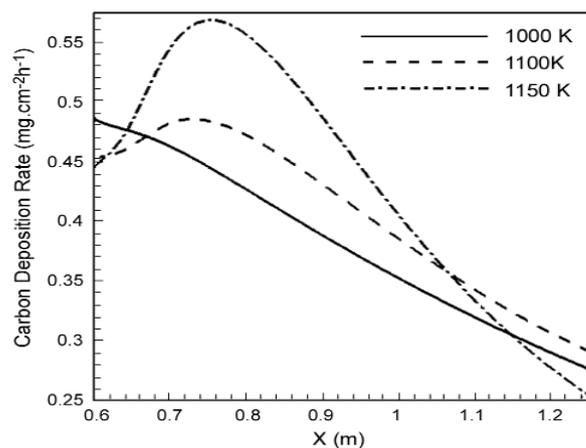**Figure 2:** *Validation with Endo et al. work [13].*

Figure 3: *Local growth rate in furnace region with different furnace temperature.*

7. RESULTS AND DISCUSSION

In this research the effects of furnace temperature and inlet hydrocarbon concentration on CNT growth rate and thickness uniformity of produced CNT has been studied. For a given inlet hydrocarbon concentration (3750 ppm) the effects of different furnace temperature on the growth rate of CNTs is shown in Figure 3. As seen, in general, CNT growth rate increases with increasing the furnace temperature. At low furnace temperature
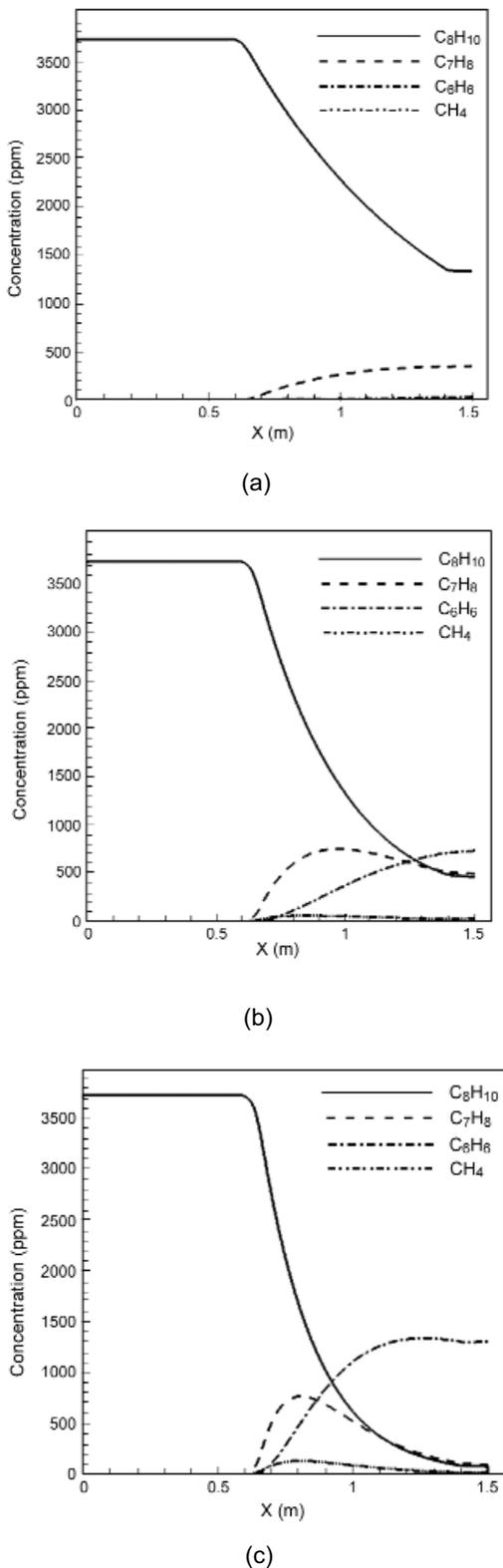
(a)

(b)

(c)

Figure 4: *Reaction product concentration throughout the reactor at different furnace temperature (a) 1000 K, (b) 1100 K and (c) 1150 K.*

(1000 K), the local growth rate monotonically decreases along the reactor length. However, for higher furnace temperature (1100 K and 1150 K) it is increased up to 0.2 m along the furnace length (between 0.6 to 0.8 meter from inlet as seen in Figure 3) then the CNT growth rate decrease with different gradient. To understand the reasons for such variations Figure 4 is presented. Figure 4 shows the effect of furnace temperature on the reactions products throughout the furnace. The balance of different products materials based on the surface reactions (Table 2) along the furnace length clearly explains the variations of the CNTs growth rate at different furnace temperature. It is known that the Arrhenius equation is used to quantify the temperature dependence of a reaction rate. Thus to better see the reason for such variations on the reactant inside of the reactor is presented (see Figure 5).
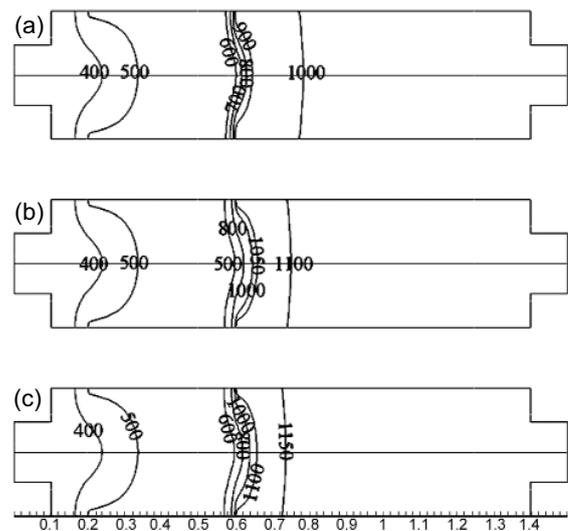

Figure 5: *Temperature distribution in reactor with different furnace temperatures (a) 1000 K, (b) 1100 K and (c) 1150 K.*

As seen in the unheated region (0 to 0.6 m) the temperature profiles are similar for different furnace temperatures. However, increasing the furnace temperature augments the reactor crosswise temperature more rapidly. The latter consumes more C_8H_{10} through a gas reaction (see Table 1)

Int. J. Bio-Inorg. Hybd. Nanomat., Vol. 2, No. 1 (2013), 329-336

Zahed Bet al

and produces more C_7H_8, C_6H_6 and CH_4. These productions, through the surface reactions causes to growth of CNTs on the catalyst layer (on the furnace wall). The contour of variations of the normalized C_8H_{10} (with inlet C_8H_{10}) is shown in Figure 6. This clearly shows the rate of C_8H_{10} consumption entire the reactor. Increasing the furnace temperature augments the rate of C_8H_{10} consumption more rapidly.
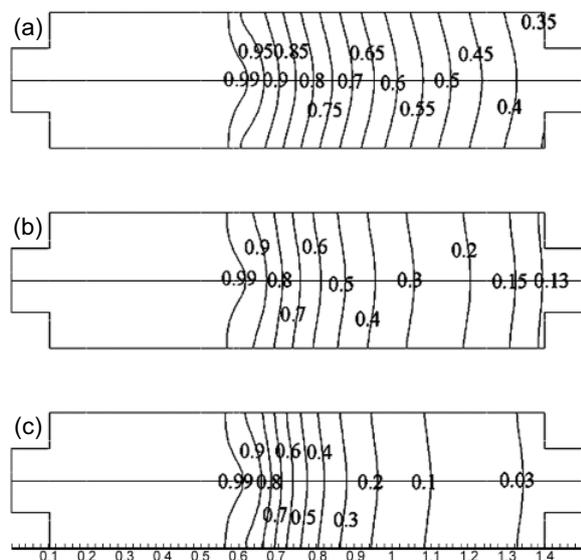

Figure 6: *Non dimensional inlet hydrocarbon (xylene) concentration in reactor with various furnace temperatures (a) 1000, (b) 1100 and (c) 1150 K.*
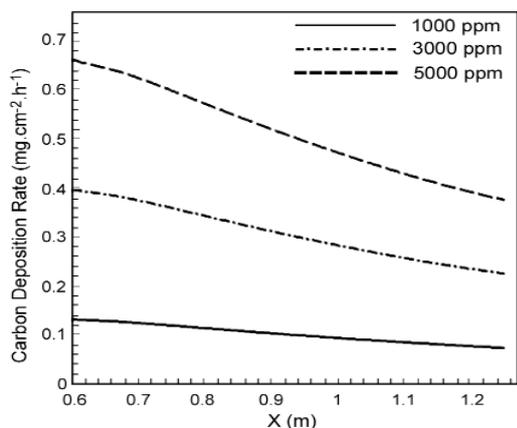

Figure 7: *Local growth rate in furnace region with different inlet hydrocarbon concentrations.*
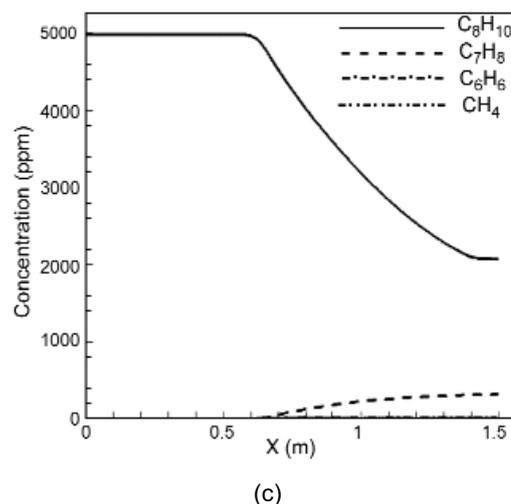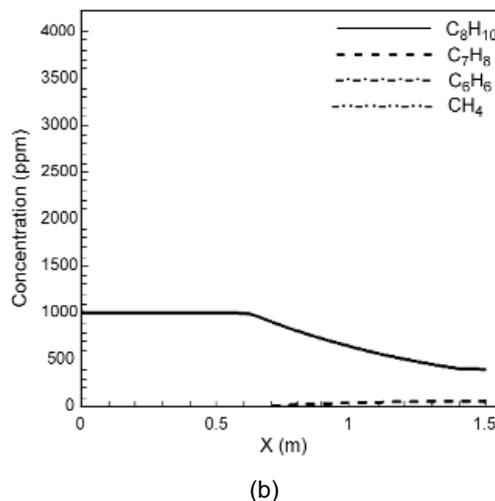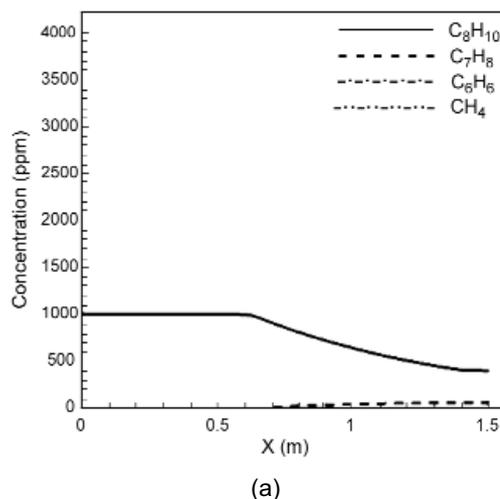

Figure 8: *Material concentrations on the reactor axis for different inlet hydrocarbon concentrations (a) 1000 ppm, (b) 3000 ppm and (c) 5000 ppm.*

To see the effects of inlet hydrocarbon concentrations on the CNTs growth rate Figure 7 is presented for a given furnace temperature (975 K). As expected by increasing the inlet hydrocarbon concentrations the rate of CNTs growth rate augments along the reactor length. However the variation of CNT growth rate along the furnace increases with the inlet hydrocarbon concentrations. It is seen that lower hydrocarbon concentrations results more uniform CNTs growth rate. This could point out that using higher concentration than the necessary amount of hydrocarbon may increase non-uniformity of the CNTs.

As seen in Figure 8 the rate of consumption and production of different materials in the reactor are similar. However, in the case of 1000 ppm of inlet hydrocarbon the amount of C_8H_{10} and C_7H_8 that exit the reactor are 400 ppm and 75 ppm respectively (Figure 8a). Increasing the inlet hydrocarbon concentration to 3000 ppm, 1300 ppm and 200 ppm of C_8H_{10} and C_7H_8 exit the reactor (Figure 8b). While for higher inlet hydrocarbon concentration (5000 ppm) 2100 ppm of C_8H_{10} and 300 ppm of C_7H_8 is remained at the reactor outlet.

8. CONCLUSIONS

CNT deposition process in an APCVD reactor was modeled and discussed. Results indicated that increasing furnace temperature has a positive effect on CNTs growth rate but decreases their uniformity. This occurrence was related to the different temperature distributions in three mentioned cases and so different material concentrations.

The effect of inlet hydrocarbon concentration on growth rate and uniformity of produced CNTs was considered also. Results showed that increasing the inlet hydrocarbon concentration leads to more growth rate due to more availability of carbon source in reactor and near reactant surfaces, particularly. In addition, increasing the inlet hydrocarbon concentration causes decreasing the CNTs uniformity due to the various carbon source consumption and productions.

REFERENCES

1. Iijima S., *Nature*, **354**(1991), 56.
2. Liang Y.X., Wang T.H., *Physica E*, **23**(2004), 232.
3. Klinke C., Afzali A., *Chem. Phys. Lett.*, **430**(2006), 75.
4. Odom T.W., Huang J.L., Kim P., Lieber C.M., *Nature*, **39**(1998), 62.
5. J. Michael, O. Connel, 2006. *Carbon nanotubes properties and applications*, New York: Taylor & Francis.
6. Lee C.J., Lyu S.C., Kim H., Park C., Yang C., *Chem. Phys. Lett.*, **359**(2002), 109.
7. Cho Y.S., Seok Choi G., Hong G.S., Kim D., *Cryst. Growth.*, **24**(2002), 224.
8. Liu W.W., Aziz A., Chai S.P., Mohamed A.R, *Physica E*, **43**(2011),1535.
9. Zahed B., Fanaei S.T., Ateshi H., *Transport Phenomena in Nano and Micro Scales*, **1**(2013), 38.
10. Andrew C.L., Chui W.K.S., *Nanotechnology*, **19**(16) (2008), 165607.
11. Pan L., Nakayama Y., Ma H., *Carbon*, **49**(2011), 854.
12. Grujicic M., Cao G., Gersten B., *J. Mater Sci.*, **38(**8) (2003), 1819.
13. Endo H., Kuwana K., Saito K., Qian D., Andrews R., Grulke E.A., *Chem. Phys. Lett.*, **387**(2004), 307.
14. Kuwana K., Saito K., *Carbon*, **43**(10) (2005), 2088.
15. Ma H., Pan L., Nakayama Y., *Carbon*, **49**(2011), 845.
16. Zhou Z.P., Ci L.J., Chen X.H., Tang D.S., Yan X.Q., Liu D.F., *Carbon*, **41**(2) (2003), 337.
17. Porro S., Musso S., Giorcelli M., Chiodoni A., Tagliaferro A., *Physica E*, **37**(1-2), (2007), 16.
18. Lin C.H., Chang H.L., Hsu C.M., Lo A.Y., Kuo C.T., *Diam Relate Mater*, **12**(10-11) (2003), 1851.
19. Bower C., Zhou O., Zhu W., Werder D.J., Jin S., *Appl. Phys. Lett.*, **77**(17) (2000), 2767.
20. Flahaut E., Govindaraj A., Peigney A., Laurent C., Rousset A., Rao C.N.R., *Chem. Phys. Lett.*, **300**(1-2) (1999), 236.

Int. J. Bio-Inorg. Hybd. Nanomat., Vol. 2, No. 1 (2013), 329-336

Zahed B et al

21. Kong J., Cassell A.M., Dai H.J., *Chem. Phys. Lett.*, **292**(4-6) (1998), 567.
22. Cassell A.M., Raymakers J.A., Kong J., Dai H., *J. Phys. Chem. B*, **103**(31) (1999), 6484.
23. Colomer J.F., Stephan C., Lefrant S., Van Tendeloo G., Willems I., Konya Z., *Chem. Phys. Lett.*, **317**(1-2) (2000), 83.
24. Hafner J.H., Bronikowski M.J., Azamian B.R., Nikolaev P., Rinzler A.G., Colbert D.T., *Chem. Phys. Lett.*, **296**(1- 2) (1998),195.
25. Che G., Lakshmi B.B., Martin C.R., Fisher E.R., Ruoff R.S., *Chem. Mater.*, **10**(1) (1998), 260.
26. Cheng H.M., Li F., Su G., Pan H.Y., He L.L., Sun X., *Appl. Phys. Lett.*, **72**(25) (1998), 3282.
27. Smith D.K., Lee D.C., Korgel B.A., *Chem. Mater.*, **8**(14) (2006), 3356.
28. Andrews R., Jacques D., Rao A.M., Derbyshire F., Qian D., Fan X., *Chem. Phys. Lett.*, **303**(5-6) (1999), 467.
29. C.L. Yaws, 1999. *Chemical Properties Handbook*, New York: McGraw-Hill.

NOMENCLATURE

C_p	Specific heat of the gas mixture ($J.kg^{-1}.K^{-1}$)
D^T	Multicomponent thermal diffusion coefficient ($kg.m^{-1}.s^{-1}$)
f	Species mole fraction
$\vec{g}$	Gravity vector
H	Molar enthalpy ($J.mole^{-1}$)
I	Unity tensor
$\vec{j}$	Diffusive mass flux vector ($kg.m^{-2}.s^{-1}$)
m_i	Mole mass of the ith species ($kg.mole^{-1}$)
$\vec{n}$	Unity vector normal to the inflow/outflow opening or wall
P	Pressure (pa)
R	Universal gas constant= 8.314 ($J.mole.K^{-1}$)
R_k	Forward reaction rate of the kth gas phase reaction ($mole.m^{-3}.s^{-1}$)
R_{-k}	Reverse reaction rate of the kth gas phase reaction ($mole.m^{-3}.s^{-1}$)

R_l^s	Reaction rate for the lth surface reaction ($mole.m^{-2}.s^{-1}$)
t	Time (s)
T	Temperature (K)
$\vec{V}$	Velocity vector ($m.s^{-1}$)

Greek Symbols

κ	Volume viscosity ($kg.m^{-1}.s^{-1}$)
λ	Thermal conductivity of the gas mixture ($W.m^{-1}.K^{-1}$)
μ	Dynamic viscosity of the gas mixture ($kg.m^{-1}.K^{-1}$)
ν_{ik}	Stoichiometric coefficient for the ith gaseous species in the kth gas phase reaction
ρ	Density ($kg.m^{-3}$)
σ_{il}	Stoichiometric coefficient for the ith gaseous species in the lth surface reaction
τ	Viscous stress tensor ($N.m^{-2}$)
ω	Species mass fraction

Subscripts

i,j	With respect to the ith/jth species

Superscripts

c	Due to ordinary diffusion
T	Due to thermal diffusion